SIMULATION OF NARROWBAND POWER LINE CARRIER COMMUNICATION FOR SMART GRID APPLICATIONS

Chandralekha Mohanachandran* **and Srinivasan Sumathi**

Received: June 28, 2021; Revised: September 29, 2022; Accepted: October 31, 2022

Abstract

For developing a reliable Power Line Carrier Communication (PLCC) system, it is extremely important to know the characteristics of different subsystems in PLCC and power lines. The circuit used to superimpose carrier signal from the transmitter with high potential power lines is termed as line tuners. The design and simulation of a capacitive type line tuner meeting IEC 60481:1974 and IEEE Std C93.4-2012 are included in this article. The wave trap allows the power signal to pass through but blocks the high-frequency carrier signal to reach terminal equipment which works at 50/60 Hertz. Three types of wave traps are studied as part of this paper: single frequency, dual frequency, and wideband wave traps. Impedance characteristics obtained in simulation show effective rejection of carrier signal as desired. The distribution power transformers are an inevitable part of the power line network which offers high attenuation to carrier signal as being inductive it functions as low pass filter. To overcome this problem a bypass circuit which could be incorporated in future power transformers is proposed in this article. The Resistance, Inductance, and Capacitance (RLC) parameter of the power line cable used in the simulation model are derived based on the experimental values observed on an actual 11 kV underground cable and thus replicates actual field conditions. A complete PLCC system with all the above components is presented in this article and can be used as a testbed by designers to validate the MODEM for communication in different topologies by modifying the elements according to actual field conditions.

Keywords: **Power line carrier communication (PLCC), Wave trap, Channel modelling, Line tuner, Underground medium-voltage cable, Attenuation, Power line channel**

Introduction

In India, PLCC technology is included by the Bureau of Indian standards (BIS) as part of its recommendation for a smart city policy. Automatic meter reading (AMR) would be one of the most sought technologies by utility companies in the near future as government materializes the plan of making 100 smart cities. The traditional electromechanical meters that we see today for electricity, water and gas would soon be replaced with smart meters which will bring cost and operational benefits to utility firms. The government's initiative to subsidize smart grid has

Electrical and Electronics Engineering Department, RNS Institute of Technology, Bengaluru 560098, India. E-mail: chandralekha85@gmail.com
* *Corresponding author*

resulted in increasing investment in smart grid solutions and hence the Narrowband PLCC (NBPLCC) is expected to lead the market in coming years as it is one of its main applications.

NBPLCC provides utility companies with a bi-directional communication platform capable of transmitting real-time data for effective management of the distribution network. NBPLCC technologies operate in the frequency band from 3 kHz to 500 kHz. There are two types of NBPLCC namely Low Data Rate (LDR) NBPLCC and High Date Rate (HDR) NBPLCC. LDR NBPLCC is capable of a few kilobytes per second (kbps) and is guided by standards like IEC 61334-3-1, IEC 61334-5-1 etc. On the other hand, HDR NBPLCC offers data rates up to 500 kilobytes per second and is guided by standards like IEC 62056-8-4, IEEE 1901.2 etc. (López *et al*., 2019).

The architecture of NBPLCC is illustrated in Figure 1. The carrier signal from the transmitter is coupled to the power line and then transmitted to the remote receiver station. During the transmission, the carrier signal is attenuated, and noise is added to the signal. At the receiver, the carrier signal is separated from the power signal in the same manner that it was coupled at the transmitter end. The carrier signal is then demodulated at the receiver station to retrieve the information. Thus, a basic PLCC system consists of terminal equipment (transmitters, receivers and control modules), coupling equipment and the PLC (Institute of Electrical and Electronics Engineers [IEEE], 2005). For building a reliable PLCC, each component of PLC must be carefully examined. To examine the performance of PLCC when integrating with field PLC components, a testbed is required.

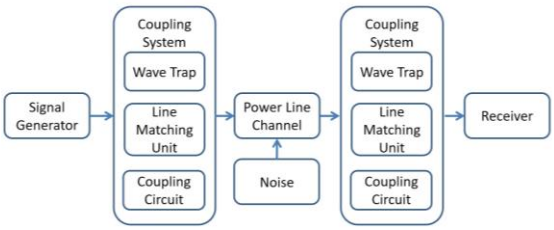

Figure 1. Block diagram of NBPLCC

The objective of this paper is to discuss the proposed NBPLCC testbed developed in the MATLAB Simulink environment. In this paper, we shall discuss how a power line carrier signal is effectively coupled to the power grid and transmitted to the destination receiver through PLC.

Manufacturers of Low Voltage (LV) and Medium Voltage (MV) cables in their datasheets specify electric parameters at 50 or 60 Hertz only, but modelling the transmission line in narrowband power line carrier communication (PLCC) application requires knowledge of per-unit length parameters for different carrier frequencies (3 kHz to 500 kHz). Thus, experimental measurement was required to determine the behaviour of the transmission line at different carrier frequencies for improving the accuracy of power line channel modelling. The narrowband carrier signal will experience high attenuation across the distribution transformer (Melit *et al*., 2012) and hence a cost-effective bypass circuit is also proposed in this work. An important aspect of this work is that, the modelling is based on guidelines specified in international standards and components used in the model are chosen from the manufacturer catalogue and hence would be appropriate in practical implementation.

To utilize a power line as a medium of communication, a coupling system is required to inject the high-frequency carrier signal without loss and at the same time protect the terminal equipment from a high voltage power line. To inject the carrier signal into the power line there are two approaches namely capacitive and inductive coupling. Capacitive coupling is mostly used in NBPLCC (International Electrotechnical Commission [IEC], 2012) and hence this paper focuses on capacitive coupling.

A capacitive coupling system consists of a wave trap with a tuning device, Coupling Capacitor (CC), a Line Matching Unit (LMU) and Drain Coil (DC).

Materials and Methods

Wave Trap

The role of the wave trap or line trap is to offer a high impedance path to the high-frequency carrier signal (30 kHz to 500 kHz) while offering a low impedance path to the power signal (50 Hz to 60 Hz). The wave trap is connected to the power line between the coupling capacitor and the substation equipment. The wave trap is also used in tap lines or branches in the transmission line to limit the attenuation of the carrier signal. Thus, a proper selection and usage of wave trap will ensure isolation of the carrier signal from the rest of the system (IEEE, 2005) and will guide the signal in the proper direction (IEEE, 2017). The requirement of wave trap is guided by the standards IEEE Std C93.3-2017, IEC 60353:1989/AMD1:2002 and IS 8792:1995 (Reaffirmed in 2006) (IEEE, 2017; IEC, 1989; Bureau of Indian Standards [BIS], 1995).

A wave trap consists of the main inductor rated to carry line current, a tuning device and a surge arrestor (IEEE, 2020; IEC, 2017). The device is connected in series with the power line between the substation and coupling capacitor and at the line taps (branches). Main coil inductance ratings in Millihenries (mH) shall be one of the following 0.265, 0.53, 1.06, 1.59, 2.12 or 2.65 according to IEEE standard C93.3-2017 (IEC, 1989). The value of wave trap inductance offered by General Electric (GE) which meets the requirement of IEC standard IEC 60353 ranges from 0.1 mH to 2.0 mH. Based on the tuning circuit, the standards define three types of wave traps namely single frequency, dual frequency and wideband wave traps.

Single Frequency Wave Trap (SFWT)

We will get a resonant circuit when a capacitor is placed in parallel to the main coil and the resulting circuit will offer high impedance at the resonant frequency. Thus, by selecting the suitable value for the main coil and capacitor we can tune it to any carrier frequency that it shall isolate. The schematic diagram from IEC and IEEE standards are shown in Figure 2(a) and Figure 2(b) respectively.

According to IEEE, for a given capacitor C_1, the circuit is tuned to resonant carrier frequency by adjusting the tap (IEEE, 2005). Whereas in IEC for a fixed main coil L_1, capacitor pack C_1 decides the tuning. Most manufacturers and utility firms prefer the IEC model wherein the tuning circuit can be replaced without removing the wave trap. The resonant frequency f_r is given by Equation (1),

$$R_{min} = k\pi L_1 \frac{f_H f_L}{f_H - f_L} \ \Omega \quad (1)$$

The frequency f_r is also the geometric mean frequency and is given by Equation (2),

$$f_r = \sqrt{f_H f_L} \quad (2)$$

In Eqs. (1) and (2), f_H is the upper-frequency band limit and f_L is the lower frequency band limit.

Resistive impedance is an inherent parameter of wave trap and is important when evaluating the high-frequency characteristic. The impedance offered by PLC components (channel, transformers etc.) can compensate for the wave trap impedance. As this is connected in series it can then form a series resonating circuit and if this resulting circuit resonates at the carrier frequency, then the entire carrier signal energy would be dissipated through sub-station equipment.

To prevent this, the tuning device shall include the minimum resistive component while manufacturing. The resistive component of blocking impedance and minimum blocking impedance of SFWT is given by Equations. (3) and (4) (GE, 2016),

$$R_{min} = k\pi L_1 \frac{f_H f_L}{f_H - f_L} \ \Omega \quad (3)$$

$$Z_{min} = \sqrt{2}\, R_{min} \ \ \Omega \quad (4)$$

In Equations. (3) and (4), R_{min} is the resistive component of blocking impedance; Z_{min} is the minimum value of blocking impedance and k is determined from the manufacturer catalogue.

MATLAB Simulink model of SFWT is realized and the characteristic impedance with respect to frequency is plotted as shown in Figures 3(a) and 3(b) respectively.

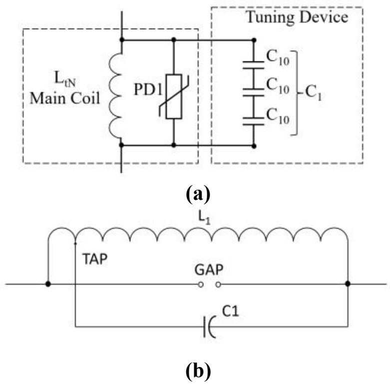

Figure 2. Circuit diagram of SFWT as per (a) IEC 60353 and (b) IEEE 643

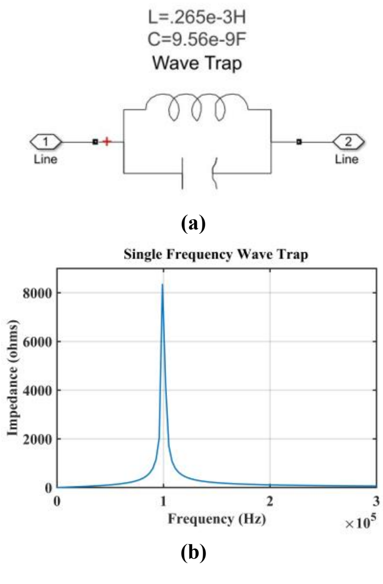

Figure 3. (a) Simulink model and (b) impedance characteristic of SFWT

Dual Frequency Wave Trap (DFWT)

DFWT is used when PLCC need to block two carrier frequencies. This is required when the transceiver uses one frequency for transmitting and another frequency for receiving or when two control modules are utilizing PLC simultaneously. The impedance peak is similar to SFWT, where there will be two resonant peaks in impedance at two different carrier frequencies. The standard specifies the separation of two resonant frequencies by 25% of higher frequency or by 25 kHz whichever is higher (IEC, 1989; IEEE, 2005). The schematic diagram from IEC and IEEE standards are shown in Figure 4(a) and Figure 4(b) respectively.

For modelling in MATLAB Simulink, the circuit in IEEE 643 standard is followed as it will enable the testbed to tune the main coil. There are three parallel resonating circuits, formed by L_1C_1, L_2C_2 and $(L_1+L_2)C_3$. Two resonant circuits L_1C_1 and L_2C_2 are tuned at higher carrier signal frequency f_H. The selection of components L_1, C_1, L_2 and C_2 is governed by Equation (5),

$$f_H = \frac{1}{2\pi\sqrt{L_1C_1}} = \frac{1}{2\pi\sqrt{L_2C_2}} \quad (5)$$

By proper selection of capacitor C_3 and setting the tap on main coil L_1, resonance at lower frequency f_L is achieved. The formula for selecting C_3 could be approximated as,

$$f_L = \frac{1}{2\pi\sqrt{(L_1+L_2)C_3}} \quad (6)$$

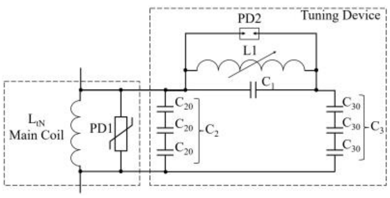

(a)

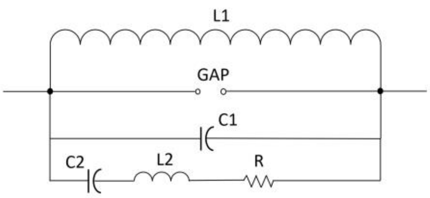

(b)

Figure 4. Circuit diagram of DFWT as per (a) IEC 60353 and (b) IEEE 643

MATLAB Simulink model of DFWT is realised and the characteristic impedance with respect to frequency is plotted as shown in Figure 5.

Wide Band Wave Trap (WBWT)

WBWT is used to block a band of carrier frequency signal. The schematic diagram from IEC and IEEE standards are shown in Figure 6(a) and Figure 6(b) respectively. For modelling in MATLAB Simulink, the circuit in IEEE 643 standard is followed. There are two resonating circuits, one parallel resonating circuit formed by L_1C_1 and a series resonating circuit formed by L_2C_2.

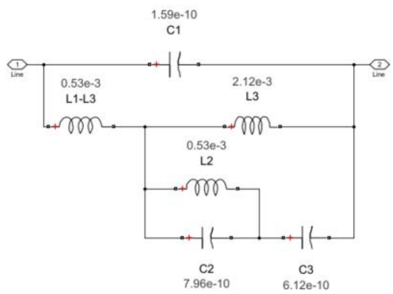

(a)

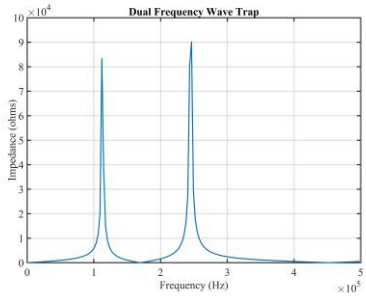

(b)

Figure 5. (a) Simulink model and (b) impedance characteristic of DFWT

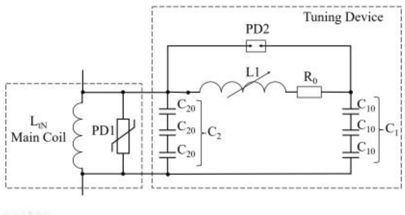

(a)

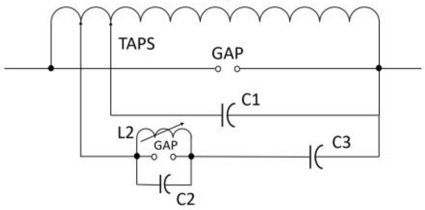

(b)

Figure 6. Circuit diagram of WBWT as per (a) IEC 60353 and (b) IEEE 643

Both resonant circuits L_1C_1 and L_2C_2 are tuned at resonant frequency f_r is given by Equation (2). Selection of components L_1, C_1, L_2, C_2 and R are governed by Equations (7) and (8),

$$f_r = \frac{1}{2\pi\sqrt{L_1C_1}} = \frac{1}{2\pi\sqrt{L_2C_2}} \tag{7}$$

$$R^2 = \omega_0{}^2 L_1 L_2 \tag{8}$$

At resonating frequency f_r, the wave trap is purely resistive with resistance R. The resistance R is called terminating resistance and is normally set to the characteristic impedance of PLC. The value of terminating resistance ranges from 400 to 1000 Ohms.

MATLAB Simulink model of WBWT is realised and the characteristic impedance with respect to frequency is plotted as shown in Figure 7.

The resistive component of blocking impedance of WBWT is given by Equation (9) (General Electric [GE], 2016).

$$R_{min} = k2\pi L_1 \frac{f_H f_L}{f_H - f_L}\ \Omega \tag{9}$$

Bandwidth, BW of WBWT is given by Equation (10) (IEEE, 2005),

$$BW = \frac{2\pi\sqrt{2}TL_1 f_r{}^2}{R} \tag{10}$$

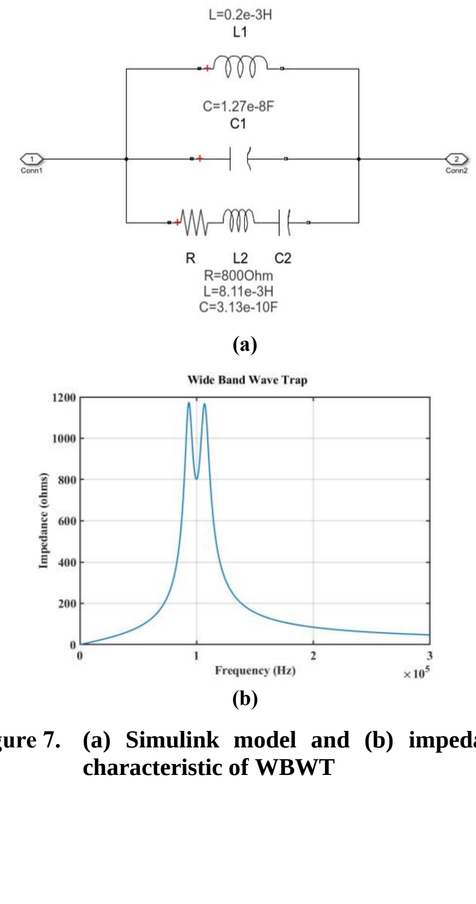

Figure 7. (a) Simulink model and (b) impedance characteristic of WBWT

In Equation (10), T is the detuning factor (approximately 0.9).

Line Tuner

For injecting the carrier signal from the transmitter to PLC, two types of coupling circuits are employed, capacitive and inductive coupling. Capacitive coupling is widely used in NBPLCC and is the focus of this work. The requirement of coupling devices used in NBPLCC is guided by standards IEC 60358:2012, IEEE Std C93.1-1999 and BIS IS 9348:1998(R2004). Effective transfer of carrier signal from transmitter/receiver to and from power line requires a set of components called line tuners. The components of a line tuner include a Coupling Capacitor (CC), an inductor in resonance with a coupling capacitor, a Blocking Capacitor (CB) and the Drain Coil (DC) (GE, 2013; Pulsar Technologies, Inc., 2013).

The schematic of the coupling circuit at the transmitter and receiver side modelled in MATLAB Simulink is shown in Figure 8. A wideband line tuning circuit is used in the model. The coupling capacitor and the line matching inductor form a series resonating circuit at carrier frequency allowing the carrier signal to pass through. The line matching inductor is varied to match the impedance between the PLCC transmitter/receiver and the PLC. Depending on the bandwidth, the LC tuning circuit will attenuate the undesired signal from other PLCCs. The series blocking capacitor protects the transmitter/receiver equipment from surge and power frequency components. The requirement of tuning devices used in NBPLCC is guided by standards IEC 60481:1974 and IEEE Std C93.4-2012.

The secondary coil of the isolation transformer is connected in parallel to the line matching inductor (L_M). In the model, the isolation transformer used is T60403-K4185-X047 of VAC® (Vacuumschmelze) make (Vacuumschmelze GmbH & Co, 2015) which offers a fixed inductance of 1.4 mH in secondary. The signal transformer provides isolation between the power line channel and carrier equipment (transmitter/receiver).

In this model, if the tuning inductance required is more than 1.4 mH then a suitable inductor may be connected in series between the blocking capacitor and the secondary of an isolation transformer. Due to the blocking capacitor, the effective capacitance of the coupling capacitor (C_{eff}) is reduced and is given by Equation (11)

$$C_{eff} = \frac{C_C C_B}{C_C + C_B} \tag{11}$$

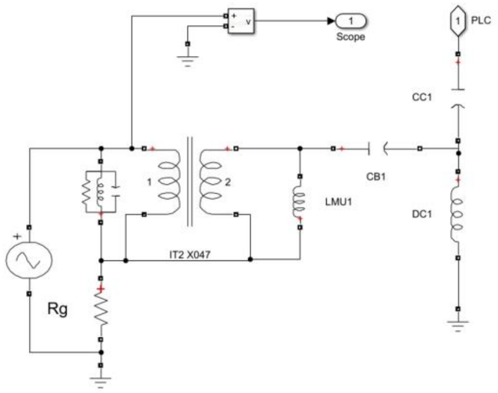

(a)

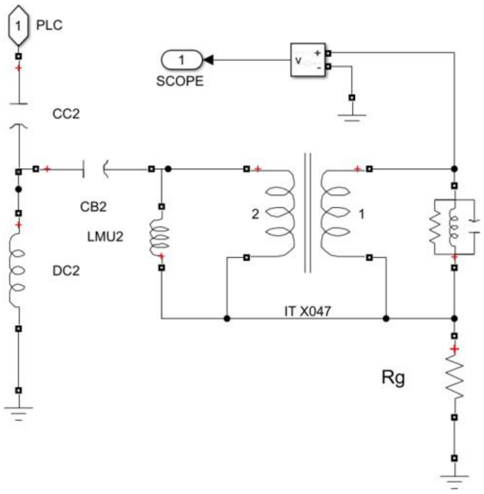

(b)

Figure 8. Simulink model of coupling circuit at (a) transmitter side and (b) receiver side

In the modelling, C_{eff} and coupling capacitance C_C is chosen as 9 nF and 13 nF respectively, and the blocking capacitor C_B is calculated by rewriting the Equation (11) as,

$$C_B = \frac{C_c C_{eff}}{C_c - C_{eff}} \quad (12)$$

The frequency to which the series resonating circuit resonate is called the geometric mean frequency (f_{gmf}) of the line matching unit and is given by Equation (13),

$$f_{gmf} = \sqrt{f_L f_H} \quad (13)$$

The inductance required to form the resonating circuit at geometric mean frequency f_{gmf} with effective coupling capacitance C_{eff} is governed by Equation (14),

$$f_{gmf} = \frac{1}{2\pi\sqrt{L_M C_{eff}}} \quad (14)$$

In the model, the parallel tuning inductance L_T is calculated by Equation (15),

$$L_T = \frac{L_M L_2}{L_2 - L_M} \quad (15)$$

In Equations. (14) and (15) L_M is the effective line matching impedance and L_2 is the secondary winding inductance of the isolation signal transformer.

The coupling capacitor and the drain coil are connected such that it forms a frequency-dependent voltage divider network. The drain coil offers a low impedance path for the power signal while offering high impedance to the high-frequency carrier signal. Thus, the drain coil protects the carrier equipment (transmitter/receiver) by grounding the power signal component appearing at the low voltage side of the coupling capacitor.

The drain coil inductance L_{DC} shall satisfy Equation (16) (IEEE, 2012),

$$L_T = \frac{L_M L_2}{L_2 - L_M} \quad (16)$$

If the value of coupling capacitance C_C is greater than 0.006 μF and if the tuning frequency (f_r) is greater than 70 kHz, the value of drain coil inductance (L_{DC}) is chosen as 10 mH. For coupling capacitance, less than 0.006 μF and tuning frequency of less than 70 kHz the inductance of the drain coil is chosen as 45 mH. Both cases satisfy Equation (16).

A very low composite loss (<1 dB) within the pass band of the coupling circuit is observed when connecting the transmitter circuit with the receiver circuit to an LV power line of short length as shown in Figure 9(a). An AC voltage source with 10 V_{P-P} is used to replicate the carrier signal. The transmitter input and receiver output waveforms are captured in Figure 9(b).

RLC (Resistance, Inductance, Capacitor) parameter used in the model is evaluated by experiment, details of which are provided in the following section.

Characterization of underground multi-conductor transmission line and experimental results

Most urban and suburban regions in the world are witnessing the conversion of overhead power lines to underground (UG) power lines to achieve a reliable and safer electricity distribution system. Thus, this work focuses on MV underground cables.

Figure 10 is taken from the actual cable, currently being laid by BESCOM as part of their esteem project involving the conversion of a 7250 km overhead power line to an underground power line for a safer and reliable power distribution system. The cable used for the experiment is 6.35/11 kV of type A2XWY with three cores of cross section 95 mm^2 and confirms to IS 7098-2(2011) (IEC, 1989; BIS, 2011). The data given in the manufacturer catalogue and obtained by physical measurement of the cable under study is given in Table 1. The core is made of aluminium wires stranded and compacted together in a circular shape; the conductor confirms IEC:60228. The core is insulated with cross-linked polyethylene (XLPE) insulating compound. XLPE insulation is applied through the extrusion process and confirms to IEC:60502. Over XLPE insulation colour strip is provided to identify core (Red, blue and yellow-R, Y & B).

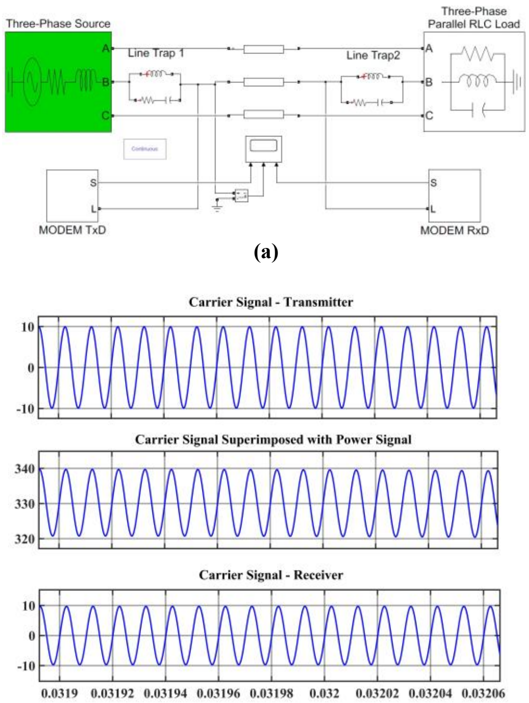

Figure 9. (a) Simulink model of coupling of the carrier signal with power line channel and its (b) waveform

Metallic shielding is provided in the form of copper taping over XLPE insulation. The three XLPE insulated and shielded cores are laid together in a cyclic-symmetric structure with polyvinyl chloride (PVC) filler. Armouring with galvanized steel wire is provided over the inner PVC filler. An outer sheath of wear and a thermal-resistant PVC compound cover the armour.

Table 1. Parameters of 11kV UG cable

Physical Parameters	
Dimension	**Value**
Overall Diameter	58 mm
Core Cross Section	95 mm^2
Number of strands	19
XLPE Thickness	3.6 mm
Copper Shield thickness	0.6 mm
Wire Armour thickness	2.5 mm
Outer PVC sheath thickness	2.5 mm
Electrical Characteristics	
Parameter	**Value**
Current rating	91 Amps
DC Resistance	0.32 Ω/km
AC resistance	0.41 Ω/km
Capacitance	0.31 µF/km
Inductance	0.38 mH/km
XLPE permittivity	2.25
PVC Sheath permittivity	4

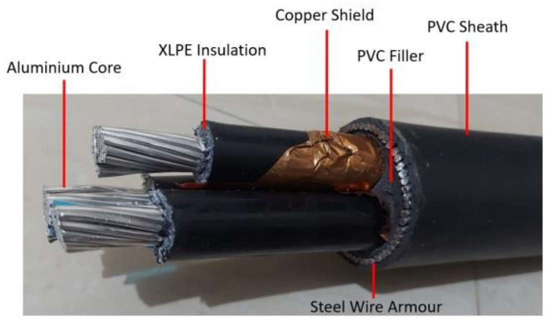

Figure 10. The cable used in the study: 6.35/11 kV A2WXY 3C X 952 mm cable

For this study, MV underground cable which is currently being laid by utility firm BESCOM (The Bengaluru electricity company) in Bengaluru, India is used. The cross-section views and marking on the cable are depicted in Figure 10. Measurement was carried out at M/s Envitest Laboratories Pvt Ltd. Bengaluru, India.

The cable under study is armoured and each core is insulated with XLPE. The cable ends were stripped to access the core for injecting and receiving the signal, refer to Figure 10. From dimensional measurement and Figure 10, the cyclic symmetry structure of the cable was confirmed. Such being the case, considering the difficulty to access the extreme ends, at one end two phases were connected together so that the signal entry and exit are brought to the same end. This way, we had an added advantage of the reduction in probe length.

The signal generator of make Wavetek, model 132 with a frequency range of 2 Hz to 2 MHz is employed to inject the signal to the PLC.

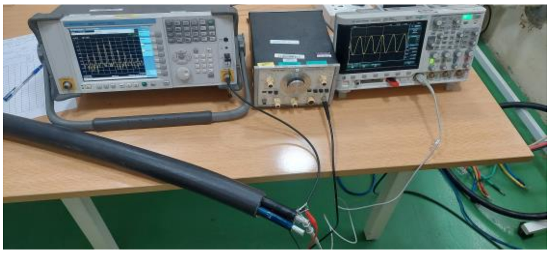

Figure 11. Measurement setup

The output terminal impedance of the signal generator is 50 Ω and a suitable 50 Ω RF cable of short length was made to connect the signal to the power line. A spectrum analyser (model N1996A) and an oscilloscope (model DSO-X 3024A) were used to record the signal that exited from the power line. The experiment setup is depicted in Figure 11.

Measurement data of resistance R, inductance L and capacitance C for the frequency range 3 kHz to 500 kHz is plotted in Figures 12(a), 12(b), and 12(c) respectively. The variation in inductance and capacitance over the narrowband frequency range is so small that it is neglected in modelling.

The experiment data of resistance is the best fit to a polynomial of second order and is given by Equation (17).

$$R(f) = -3e^{-6}f^2 + 3.5e^{-3}f + 0.4541 \quad (17)$$

The simulation of PLC is modelled as shown in Figure 9(a) with the RLC parameter set to the value observed by measurement. The simulation model is validated by comparing the attenuation measured by experiment and that obtained by simulation. The attenuation was evaluated using the formula,

$$\propto = \left|20\log\left(\frac{V_{out}}{V_{IN}}\right)\right| \quad (18)$$

where V_{out} is the voltage leaving the power line, while V_{IN} is the voltage injected in the power line. Figure 13 shows the comparison of attenuation obtained in the Simulink model and by experimental measurement with and without probe compensation. From the plot, after probe compensation, the measured attenuation is in good agreement with the attenuation observed in the simulation model.

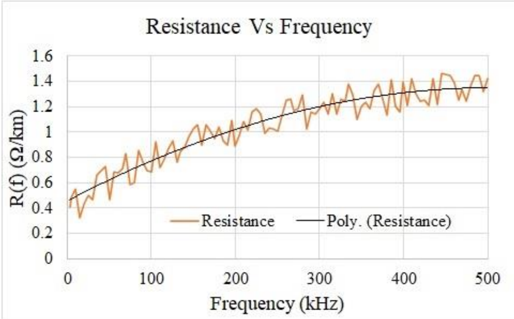

(a)

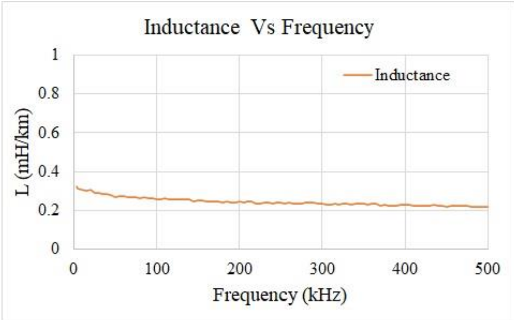

(b)

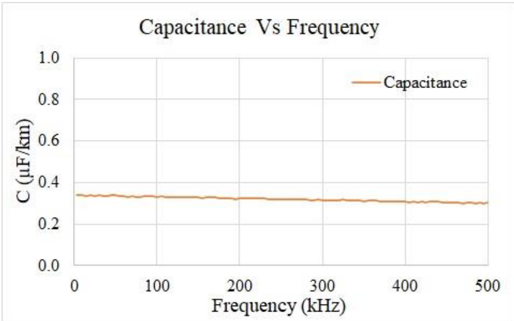

(c)

Figure 12. Measurement result of (a) Resistance (b) Inductance and (c) Capacitance for different frequencies.

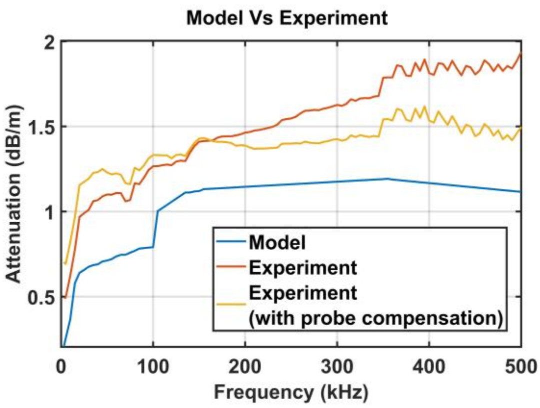

Figure 13. Attenuation observed in simulation model vs experiment

Results and Discussion

The flow chart of the simulation model is given in figure 14 based on which power line channel as prescribed in IEEE 1901.2 standard (IEEE, 2013; IEEE, 2015) is modelled as shown in Figure 15. At the analogue front end of the digital modem, the baseband modulated signal is mixed with the carrier signal which forms the modulated carrier signal. A sine wave generator with 10 volts peak to peak is used in the model to replicate the modulated carrier signal. The next step is to inject this high-frequency carrier signal into the power line which is at high voltage. So, the design of the coupling device shall offer protection to the modem from high voltage components in the power line but at the same time shall efficiently inject the carrier signal to the power line. A series blocking capacitor and signal isolation transformer used in the model protect the modem from surges, and power frequency component and provides perfect isolation between the power line channel and carrier equipment. Capacitive coupling guided by standards IEC 60358:2012, IEEE Std C93.1-1999 and BIS IS 9348:1998(R2004) is used in the model. A line matching inductor is incorporated in the model for impedance matching between modem and power line channel. The coupling capacitor and the line matching inductor form a series LC tuning circuit resonating at the carrier frequency. In addition, a drain coil is connected at the low voltage side of the coupling capacitor which offers a low impedance path to the power signal and protects the modem by grounding the power signal component appearing at the low voltage side of the coupling capacitor.

The Coupling Capacitor (CC), line matching inductor in resonance with the coupling capacitor, a Blocking Capacitor (CB) and the Drain Coil (DC) together forms the line tuner and made it into a sub-system and named Modem TxD in the model.

The same circuit is employed at the receiver end except for the signal generator. It is replaced with scope to view the received signal; the sub-system is named Modem RxD. The design details and parameter used in the model is detailed under the heading “Line Tuner” in this article.

In the simulation model, the transmitter (Modem TxD) and receiver (Modem RxD) are positioned to simulate LV to MV to LV communication channel. A three-phase generator is employed as a distributed energy resource. From the source, through MV lines the power will reach the substations where it is stepped down to LV and through LV lines the power reaches the end user for consumption. The power line cable RLC parameters were evaluated through experiment and are used in the model. Line trap circuits are employed for loads and generators to block high-frequency carrier signals thereby guiding the carrier signal to the receiver. The distribution transformer is a low-pass filter that attenuates the carrier signal almost completely as it acts like a wave trap. For effective transmission of the carrier signal from LV to MV, a two-way bypass circuit as shown in Figure 16(a) was connected across the distribution transformer. With the bypass circuit connected across distribution transformers and by proper tuning of the coupling circuit, the power line carrier signal is effectively coupled to the power grid and transmitted to the destination receiver through PLC and the waveforms are captured in Figure 16(b).

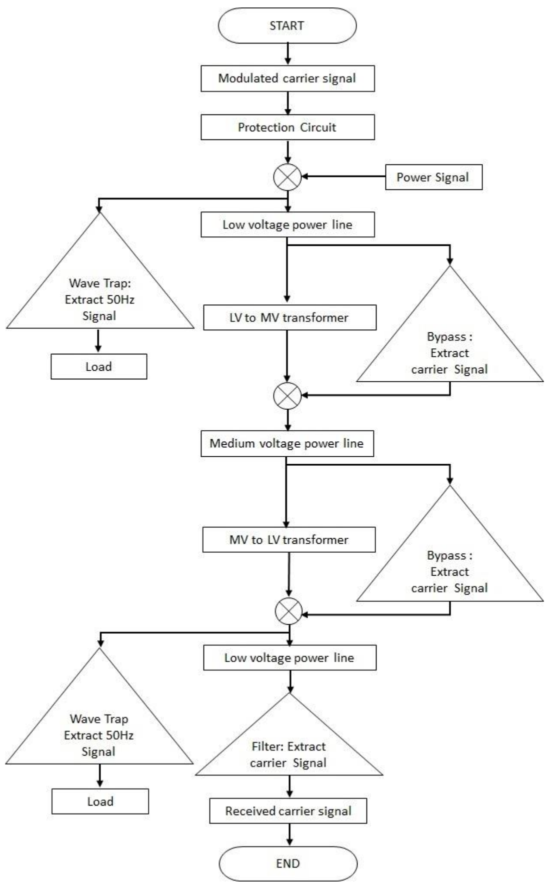

Figure 14. Flowchart of simulation model

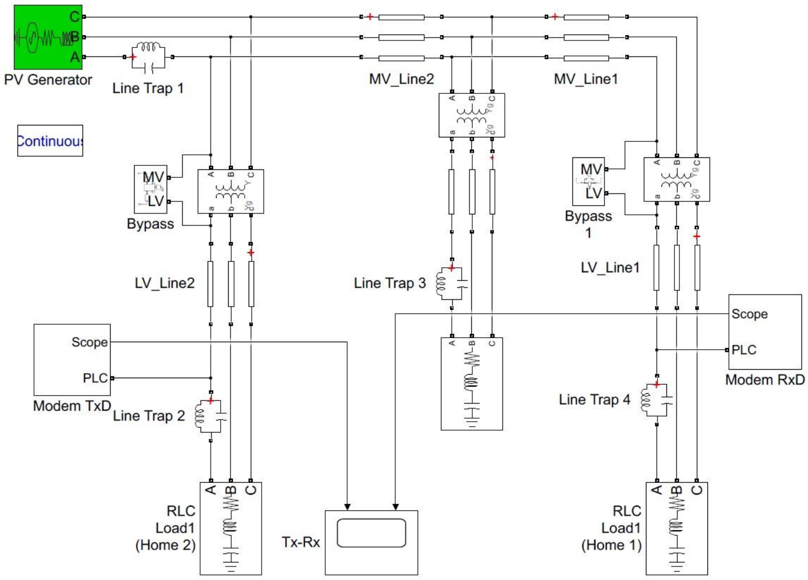

Figure 15. Model of power line channel as prescribed in IEEE 1901.2 standard: LV to MV to LV

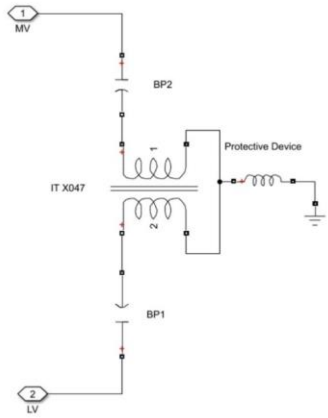

(a)

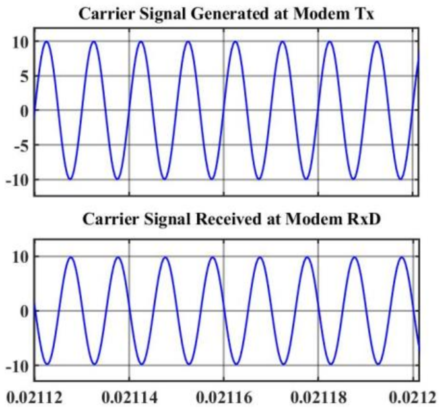

(b)

Figure 16. (a) Bypass circuit for LV/MV distribution transformer; (b) Waveform of LV to MV to LV using transformer bypass circuit

Conclusions

The design of three types of wave traps: single frequency, dual frequency and wideband wave traps and their respective impedance characteristic with respect to frequency is presented in this paper. The selection of the type and the parameters of the wave trap depends on the carrier frequency with which the modem operates. The line tuner presented in this article provides protection circuits needed for the safe operation of the modem when working with a high potential power line as a communication medium. For maximum power transfer between the modem and the power line, the line matching inductor is tuned to match the line impedance as in the actual field. The RLC parameter of the power line used in the model is based on values from experimental observation. The distribution transformers in the power line network are the main limiting factor for power line communication technology to cover the distance. A transformer bypass circuit is proposed to overcome this issue. The bypass circuit proposed could be incorporated inside the future transformer which will reduce the cost and widens the communication network. The system presented in this article is modelled in MATLAB Simulink environment and has all the components needed for power line carrier communication. The designers can use this model as a testbed to validate their modem designs by modifying the power line channel according to the field data.

Acknowledgements

The authors are thankful to Dr. M.K. Venkatesha, Principal, RNS Institute of Technology, Bengaluru, India for the support he rendered for the fulfilment of this paper and M/s Envitest Laboratories Pvt Ltd. Bengaluru, India for providing facilities to conduct the experiment.

References

Bureau of Indian Standards [BIS]. (2011). Crosslinked Polyethylene Insulated Thermoplastics Sheathed Cables, Part 2: for Working Voltages from 3.3 kV up to and Including 33 kV. ETD 09: Power Cables Sectional Committee, New Delhi, IS 7098 (Part 2): 2011. 14p. Available from: www.bis.gov.in.

Bureau of Indian Standards [BIS]. (1995). Line traps for AC power systems specification. LITD 10: Power System Control and Associated Communications, New Delhi, IS 8792: 1995. 11p. Available from: www.bis.gov.in.

General Electric Company [GE]. (2016). Line Traps - air core, dry type up to 800 kV. GE Grid Solutions, Ontario, GRID-AIS-L3-LineTraps-0247-201510-EN. 8p. Available from: www.gegridsolutions.com.

General Electric Company [GE]. (2013). Relaying Communication Channels: Application guide. GE Power Management, Ontario, GET-8034. 442p. Available from: www.GEindustrial.com/pm.

International Electrotechnical Commission [IEC]. (1989). Line traps for a.c. power systems. TC 57 - Power systems management and associated information exchange, Geneva, IEC 60353: 1989. 79p. Available from: www.iec.ch.

International Electrotechnical Commission [IEC]. (2012). Power line communication systems for power utility applications - Part 1: Planning of analogue and digital power line carrier systems operating over EHV/HV/MV electricity grids. TC 57 - Power systems management and associated information exchange, Geneva, IEC 62488-1:2012. 262p. Available from: www.iec.ch.

International Electrotechnical Commission [IEC]. (2017). Surge arresters - Part 8: Metal-oxide surge arresters with external series gap (EGLA) for overhead transmission and distribution lines of a.c. systems above 1 kV. TC 37 - Surge arresters, Geneva, IEC 60099-8:2017. 138p. Available from: www.iec.ch.

Institute of Electrical and Electronics Engineers [IEEE]. (2005). IEEE Guide for Power-Line Carrier Applications. Power System Communications Committee, New York, IEEE Std 643-2004. 140p. Available from: www.ieee.org.

Institute of Electrical and Electronics Engineers [IEEE]. (2015). IEEE Standard for Low-Frequency (less than 500 kHz) Narrowband Power Line Communications for Smart Grid Applications - Amendment 1. Power Line Communications Standards Committee, New York, IEEE Std 1901.2a-2015. 28p. Available from: www.ieee.org.

Institute of Electrical and Electronics Engineers [IEEE]. (2013). IEEE Standard for Low-Frequency (less than 500 kHz) Narrowband Power Line Communications for Smart Grid Applications. Power Line Communications Standards Committee, New York, IEEE Std 1901.2-2013. 269p. Available from: www.ieee.org.

Institute of Electrical and Electronics Engineers [IEEE]. (2020). IEEE Standard for Metal-Oxide Surge Arresters for AC Power Circuits (>1 kV). Surge Protective Devices Committee, New York, IEEE Std C62.11-2020. 120p. Available from: www.ieee.org.

Institute of Electrical and Electronics Engineers [IEEE]. (2013). IEEE Standard for Power-Line Carrier Line-Tuning Equipment (30 kHz to 500 kHz) Associated with Power Transmission Lines. Power System Communications Committee, New York, IEEE Std C93.4-2012. 67p. Available from: www.ieee.org.

Institute of Electrical and Electronics Engineers [IEEE]. (2017). IEEE Standard Requirements for Power-Line Carrier Line Traps (30 kHz to 500 kHz). IEEE Power and Energy Society, New York, IEEE Std C93.3-2017. 46p. Available from: www.ieee.org.

López, G., Matanza, J., De La Vega, D., Castro, M., Arrinda, A., Moreno, J. I., and Sendin, A. (2019). The Role of Power Line Communications in the Smart Grid Revisited: Applications, Challenges, and Research Initiatives. IEEE Access, 7(1):117346-117368. https://doi.org/10.1109/ACCESS.2019.2928391

Melit M., Nekhoul B., Sekki, D., and Kerroum K. (2012). Modelling of the transmission of power line communication signal trough the power electric transformer. Annals of Telecommunications (Springer), 67(9-10):447-454. https://doi.org/10.1007/s12243-011-0277-4

Pulsar Technologies, Inc., (Canada). (2013). Power line carrier channel and application considerations for transmission line relaying. AMETEK Power Instruments, New York, C045–P0597. 49p. Available from: www.ametekpower.com.

Vacuumschmelze GmbH and Co, (Germany). (2015). Isolation transformer for narrowband PLC systems. VACUUMSCHMELZE ADVANCED MAGNETIC SOLUTIONS, Hanau, T60403-K5024-X044. 3p. Available from: www.vacuumschmelze.com.